LETTER

doi:10.1038/nature10889

DNA-based self-assembly of chiral plasmonic nanostructures with tailored optical response

Anton Kuzyk[1]*†, Robert Schreiber[2]*, Zhiyuan Fan[3], Günther Pardatscher[1], Eva-Maria Roller[2], Alexander Högele[2], Friedrich C. Simmel[1], Alexander O. Govorov[3] & Tim Liedl[2]

Matter structured on a length scale comparable to or smaller than the wavelength of light can exhibit unusual optical properties[1]. Particularly promising components for such materials are metal nanostructures, where structural alterations provide a straightforward means of tailoring their surface plasmon resonances and hence their interaction with light[2,3]. But the top-down fabrication of plasmonic materials with controlled optical responses in the visible spectral range remains challenging, because lithographic methods are limited in resolution and in their ability to generate genuinely three-dimensional architectures[4,5]. Molecular self-assembly[6,7] provides an alternative bottom-up fabrication route not restricted by these limitations, and DNA- and peptide-directed assembly have proved to be viable methods for the controlled arrangement of metal nanoparticles in complex and also chiral geometries[8–14]. Here we show that DNA origami[15,16] enables the high-yield production of plasmonic structures that contain nanoparticles arranged in nanometre-scale helices. We find, in agreement with theoretical predictions[17], that the structures in solution exhibit defined circular dichroism and optical rotatory dispersion effects at visible wavelengths that originate from the collective plasmon–plasmon interactions of the nanoparticles positioned with an accuracy better than two nanometres. Circular dichroism effects in the visible part of the spectrum have been achieved by exploiting the chiral morphology of organic molecules and the plasmonic properties of nanoparticles[18–20], or even without precise control over the spatial configuration of the nanoparticles[12,21,22]. In contrast, the optical response of our nanoparticle assemblies is rationally designed and tunable in handedness, colour and intensity—in accordance with our theoretical model.

To demonstrate the potential of DNA origami for the programmable and nanometre-precise design of plasmonic nanostructures, we targeted an optical response that emerges as a collective effect from spatially precisely arranged multiple nanoparticles in close proximity, and that requires genuinely three-dimensional structures. The response of helically arranged metallic nanocrystals to an electromagnetic field meets both criteria. Much like the circular dichroism (CD, the differential absorption of left and right circularly polarized light) effect seen with 'optically active' chiral molecules such as DNA and proteins that exhibit CD in the ultraviolet and infrared ranges owing to the electronic and vibronic excitations of their chiral secondary structure[23], strong CD signals in the visible spectrum have been predicted to occur through collective Coulomb interaction of plasmonic dipoles in chiral assemblies of metal nanoparticles[17]. (See Supplementary Information notes 1 and 2 for information on naturally occurring CD, and on the theoretical framework of plasmon-induced CD.)

To create helical nanoparticle assemblies, we used the DNA origami[15,16] approach where hundreds of rationally designed 'staple' oligonucleotides are hybridized to a long single-stranded DNA scaffold to force it into a specific two- or three-dimensional shape. The resulting objects are fully addressable by their DNA sequence, enabling further decoration and functionalization in a unique, sequence-specific manner[24]. Geometrical and material parameters can be tailored by simple adjustments of the design and fabrication protocols, which should make it feasible to quantitatively tune the optical activity of such nanostructures dispersed in solution.

Figure 1a illustrates the nanostructure design (design details and DNA sequences are given in Supplementary Information note 3). It is based on DNA origami 24-helix bundles that offer nine helically arranged attachment sites for plasmonic particles coated with single-stranded DNA, here gold nanoparticles with a diameter of 10 nm. By using nanoparticles covered with multiple linker strands, we can avoid yield-lowering purification procedures and instead add an excess of modified gold particles for hybridization to the DNA structures; unconjugated gold particles are simply removed for re-use in later experiments. The quality of the assemblies was assessed by transmission electron microscopy (TEM) (Fig. 1b) (experimental details and additional TEM images can be found in Supplementary Information note 4). The strength of the optical activity critically depends on the quality of the assembled structures[25], so we improved our experimental protocol to achieve a nanoparticle attachment yield of 96% and 98% per site and an overall yield of 77% and 86% of perfect assemblies of right- and left-handed helices with nine nanoparticles, respectively (Supplementary Information note 5). Most of the imperfect structures exhibited only a single defect within an otherwise well-formed helix. Helices stored for three months at 4 °C were still intact (Supplementary Information note 6). As illustrated in Fig. 1c, CD measurements were then carried out on solutions containing left- or right-handed nanohelices.

Left-handed helical arrangements of plasmonic particles are expected to produce a CD signal with a characteristic bisignate peak–dip shape, with the peak centred around the plasmon resonance frequency. Right-handed helices should produce a vertically mirrored dip–peak signal. Indeed, CD spectra measured on samples with gold nanoparticle assemblies of both helicities exhibited the anticipated signatures (Fig. 2a). These responses arise because the helical arrangement of the gold nanoparticles results in coupled plasmon waves propagating along a helical path and causing increased absorption of those components of the incident light that are in accord with the handedness of the helices. The bisignate appearance of the CD signals results from the isotropic nature of our samples, in which the nanohelices are randomly oriented with respect to the direction of the incident light. The interactions between the individual gold particles within each helix create a splitting between the longitudinal and transverse modes of the electromagnetic wave, and these modes typically have opposite chirality. As a result, the plasmonic CD spectrum acquires the characteristic dip–peak shape (Supplementary Information note 2).

[1]Physik Department and ZNN/WSI, Technische Universität München, Am Coulombwall 4a, 85748 Garching, Germany. [2]Fakultät für Physik and Center for Nanoscience, Ludwig-Maximilians-Universität, Geschwister-Scholl-Platz 1, 80539 München, Germany. [3]Department of Physics and Astronomy, Ohio University, Athens, Ohio 45701, USA. †Present address: Department of Applied Physics, Aalto University School of Science, FI-00076 Aalto, Finland.
*These authors contributed equally to this work.

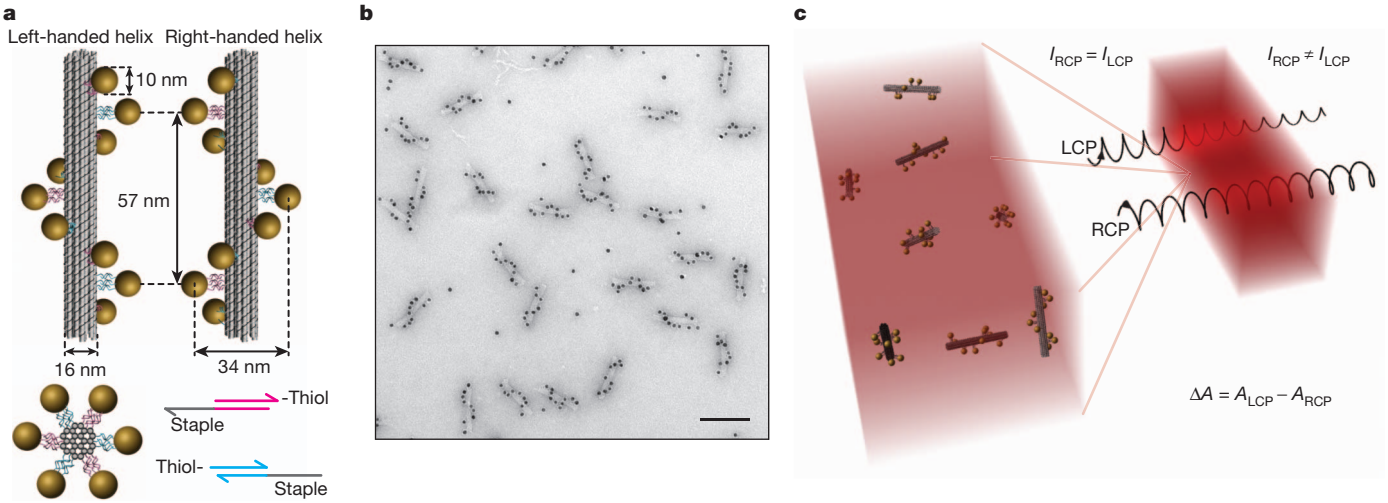

Figure 1 | Assembly of DNA origami gold nanoparticle helices and principle of circular dichroism. **a**, Left- and right-handed nanohelices (diameter 34 nm, helical pitch 57 nm) are formed by nine gold nanoparticles each of diameter 10 nm that are attached to the surface of DNA origami 24-helix bundles (each of diameter 16 nm). Each attachment site consists of three 15-nucleotide-long single-stranded extensions of staple oligonucleotides. Gold nanoparticles carry multiple thiol-modified DNA strands, which are complementary to these staple extensions. Nanoparticles and 24-helix bundles are mixed for assembly and the resulting constructs are gel-purified. **b**, TEM image of assembled left-handed gold nanohelices (scale bar, 100 nm). Analysis of the TEM data yields a 98% success rate for directed attachment of nanoparticles. **c**, Circular dichroism is measured as the difference in absorbance $\Delta A = A_{LCP} - A_{RCP}$ of left-hand-circularly polarized (LCP) and right-hand-circularly polarized (RCP) light as a function of wavelength. CD measurements were performed with a CD spectrometer on samples in cuvettes of optical path length 3 mm.

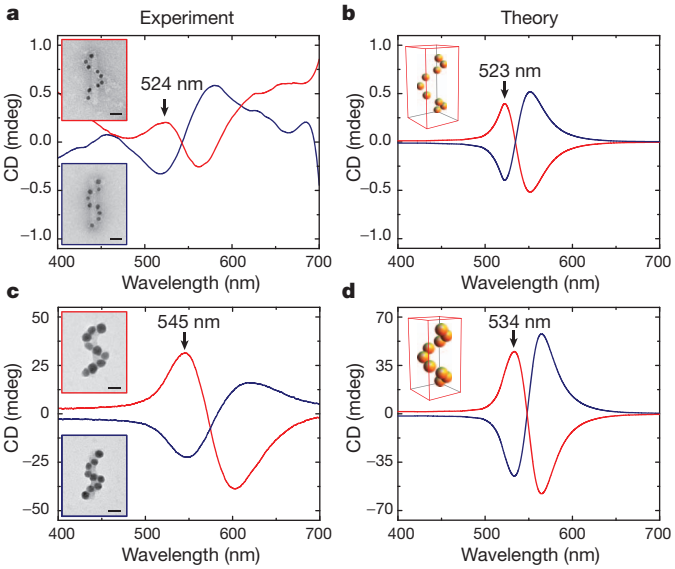

Figure 2 | Circular dichroism of self-assembled gold nanohelices. Experimental (**a** and **c**) and theoretical (**b** and **d**) CD spectra of left-handed (red lines) and right-handed (blue lines) helices of nine gold nanoparticles show characteristic bisignate signatures in the visible. **a**, CD spectra of nanohelices composed of 10-nm gold particles. The peak position in the spectra of left-handed helices (indicated by the arrow) coincides with the plasmon absorption resonance maximum. **b**, The theoretically predicted CDs for the geometries in **a** exhibit the same features; the peak positions and amplitudes are in remarkable agreement with the experiment. **c**, The CD signal increases owing to collective plasmonic enhancement by a factor of 400 for assemblies of nanoparticles with 16-nm diameter, rendering the noise in the spectra invisible (as in **a**). The peak position for left-handed helices exhibits a red-shift from 524 nm to 545 nm. **d**, The corresponding theoretical calculation predicts a 500-fold enhancement of the signal and a peak shift from 523 nm to 534 nm. The CD spectra were recorded at concentrations of nanohelices of 1.5 nM in **a** and 0.4 nM in **c**. The insets in **a** and **c** show TEM images of left-handed (red frame) and right-handed (blue frame) nanohelices (scale bars, 20 nm); the respective left-handed model geometries are depicted in the insets to **b** and **d**.

The experimental spectra agree well with theoretical calculations based on classical electrodynamics (Fig. 2b). The strongest absorption of circularly polarized light is predicted in the vicinity of the surface plasmon frequency of the metal nanoparticles, as experimentally seen with our assemblies. Strikingly, even the strength of the measured signals closely matches the magnitude predicted by the calculations. We further confirmed theoretically that the CD signal remains robust to positional perturbations of the individual particles (see Supplementary Information note 2).

The dipole theory[17] predicts that the CD signal becomes stronger when the particles are either larger or arranged in a tighter helix:

$$\mathrm{CD}_{\mathrm{plasmon}} \approx \frac{a_{\mathrm{NP}}^{12}}{R_0^8} \qquad (1)$$

where a_{NP} and R_0 are the nanoparticle and helix radii, respectively. We quantified the influence of particle size on the CD signal by using electroless deposition of metal from solution[26,27] onto 10-nm seeding particles that were already assembled into the helical geometry described in Fig. 1 (see Supplementary Information note 7 for experimental details and additional TEM images). CD measurements of these 'enhanced' samples showed two notable effects (Fig. 2c): the signal strength increased up to 400-fold for nanoparticle diameters of 16 ± 2 nm, and the absorption as well as the CD peak shifted to longer wavelengths. These results are consistent with theoretical predictions for the plasmonic CD effect. A simple estimate for the CD signal increase based on equation (1) and assuming a particle size of 16 nm yields an enhancement of about 280, and quantitative numerical calculations predict an enhancement of about 500. As in the experiments, the calculated CD for larger particles and the same helix radius is also red-shifted (Fig. 2d), which is typical for strongly interacting plasmonic nanocrystals[28]. Taken together, these observations illustrate that desired optical behaviour can be designed and realized by exploiting the collective interactions between plasmonic particles attached with close to 100% yield and positioned with nanometre-scale precision.

To generate CD at other wavelengths, we plated silver onto pre-assembled 10-nm gold particle helices and thereby produced a silver shell of about 3 nm around each of the gold nanoparticles. Plasmon resonances in silver occur at a shorter wavelength than in gold, so the

recorded CD spectra were shifted into the blue spectral region (Fig. 3a). To fine-tune the optical response to intermediate wavelengths, we used mixtures of gold and silver ions in the plating solution to grow alloy shells around the seed particles. Figure 3a presents a TEM image (upper inset) with the corresponding CD spectrum of an alloy-coated structure. As expected, the CD signal for the alloy helices appears at an intermediate wavelength (absorption spectra and additional CD spectra are presented in Supplementary Information note 8). Mixing of solutions containing different types of structures resulted in a linear superposition of the corresponding spectra (Fig. 3a). These experiments indicate the potential of our assembly method for the fabrication of optically active materials with customized spectral response.

To visualize the collective optical activity of our self-assembled nanohelices in a macroscopic optical experiment, we exposed gold nanoparticle helices to excessive amounts of silver ions during electroless metal deposition and thereby achieved a giant molar CD of around $10^8\,M^{-1}\,cm^{-1}$. The corresponding spectra are presented in Fig. 3b. Droplets of samples containing left-handed or right-handed helices and a non-helical control droplet were placed onto a glass slide between two linear polarizers. As demonstrated in Fig. 4 with polarization-resolved transmission images, the droplets with gold helices rotate the polarization angle of the linearly polarized light. Although our set-up is insensitive to polarization below 550 nm, rotation of the polarization axis of the linearly polarized light was detected for both right- and left-handed helices in the red band of the visible spectrum. The observation is in accordance with the effect of optical rotatory dispersion, which is characteristic of chiral materials exhibiting CD. In the case of our right-handed "metafluid"[29], the polarization axis is rotated clockwise (or counter-clockwise) at wavelengths above (or below) 560 nm; the opposite effect is seen with the left-handed nanohelices. The control sample containing isotropically dispersed 10-nm gold nanoparticles exhibited no such optical activity. Further details on the materials characteristics (anisotropy factor and specific rotation) can be found in Supplementary Information notes 8 and 9.

In future experiments we will explore the possibility of realizing materials with a negative refractive index without the requirement of either ε or μ being negative[30], using fluids with oriented or densely packed plasmonic helices, which should lead to a further increase of the chiral optical response. But irrespective of whether this goal can be realized, the present findings clearly establish DNA origami as a valuable addition to the existing tools at the material engineer's disposal for precisely arranging nanoparticles into assemblies with desired electric or magnetic properties.

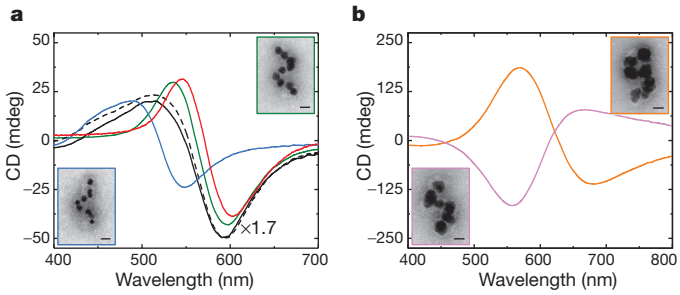

Figure 3 | Spectral tuning of circular dichroism by metal composition. **a**, A pronounced blueshift of the peak position in the CD response was achieved by depositing several nanometres of silver on gold nanoparticles of diameter 10 nm (blue spectrum of left-handed gold-core/silver-shell nanohelices; red spectrum from Fig. 2c is shown for reference). Growth of silver+gold alloy shells gives rise to an intermediate blueshift (green spectrum of left-handed gold-core/silver+gold-shell helices). Mixing of solutions that contain nanohelices of various metal compositions results in a superposition of individual CD responses (black spectrum): a 2:3 mixture of gold-core/silver-shell (blue spectrum) and gold-core/silver+gold-shell (green spectrum) exhibits CD close to the predicted superposition (dashed black line; black curves were rescaled by a factor of 1.7 for presentation purposes). **b**, Excessive metal deposition leads to the merging of nanoparticles and further enhancement of the CD signal for the left-handed (orange spectrum) and right-handed (purple spectrum) gold-core/silver-shell helices. The corresponding molar CD in the visible spectrum is huge with a strength of about $10^8\,M^{-1}\,cm^{-1}$. The CD spectra were recorded at concentrations of nanohelices of 0.4 nM in **a** and 40 pM in **b**. The insets in **a** and **b** show TEM images of left-handed (blue, green and orange frames) and right-handed (purple frame) nanohelices (scale bars, 20 nm).

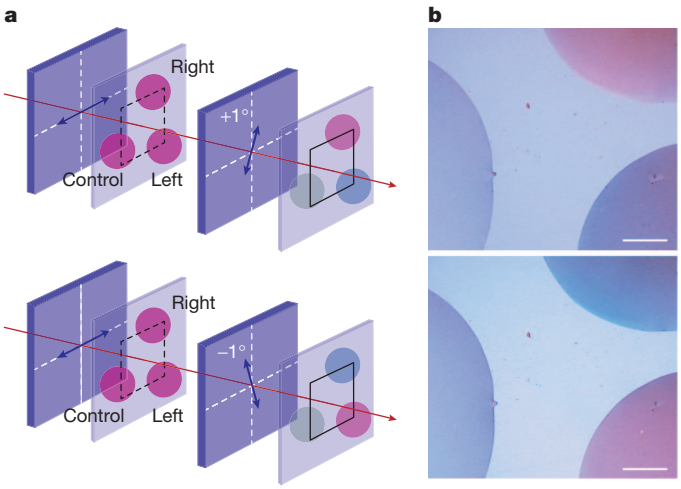

Figure 4 | Optical rotatory dispersion of self-assembled gold nanohelices. **a**, The macroscopic optical activity of the metafluid is demonstrated in polarization-resolved transmission by placing droplets of left-handed and right-handed nanohelices as well as a control droplet with isotropically dispersed gold nanoparticles between two linear polarizers. The components of the transmission set-up are ordered along the propagation path of white light as follows: linear polarizer, sample, linear analyser, screen (charge-coupled-device camera). The extinction characteristics of the linear polarizers render the set-up polarization-insensitive for wavelengths below 550 nm. **b**, Real-colour transmission images (scale bar, 1 mm) of the droplets for clockwise (top) and counter-clockwise (bottom) rotation of the analyser by one degree out of the orthogonal configuration. The droplets of right-handed and left-handed helices appear red in the top and bottom images, respectively, as a result of optical rotatory dispersion. Right- (or left-) handed nanohelices rotate the polarization axis of the transmitted light in positive (or negative) and negative (or positive) directions in the red and blue spectral bands, respectively. The rotation of the polarization in the red band is sensitively detected by the set-up, but green and blue components of white light illumination (below 550 nm) are not polarization-resolved and contribute only to the bluish background.

Received 12 September 2011; accepted 17 January 2012.

1. Liu, Y. & Zhang, X. Metamaterials: a new frontier of science and technology. *Chem. Soc. Rev.* **40,** 2494–2507 (2011).
2. Barnes, W. L., Dereux, A. & Ebbesen, T. W. Surface plasmon subwavelength optics. *Nature* **424,** 824–830 (2003).
3. Polman, A. Plasmonics applied. *Science* **322,** 868–869 (2008).
4. Soukoulis, C. M. & Wegener, M. Past achievements and future challenges in the development of three-dimensional photonic metamaterials. *Nature Photon.* **5,** 523–530 (2011).
5. Gansel, J. K. *et al.* Gold helix photonic metamaterial as broadband circular polarizer. *Science* **325,** 1513–1515 (2009).
6. Jones, M. R., Osberg, K. D., Macfarlane, R. J., Langille, M. R. & Mirkin, C. A. Templated techniques for the synthesis and assembly of plasmonic nanostructures. *Chem. Rev.* **111,** 3736–3827 (2011).
7. Fan, J. A. *et al.* Self-assembled plasmonic nanoparticle clusters. *Science* **328,** 1135–1138 (2010).
8. Seeman, N. C. Nanomaterials based on DNA. *Annu. Rev. Biochem.* **79,** 65–87 (2010).
9. Tan, S. J., Campolongo, M. J., Luo, D. & Cheng, W. Building plasmonic nanostructures with DNA. *Nature Nanotechnol.* **6,** 268–276 (2011).
10. Ding, B. *et al.* Gold nanoparticle self-similar chain structure organized by DNA origami. *J. Am. Chem. Soc.* **132,** 3248–3249 (2010).
11. Mastroianni, A. J., Claridge, S. A. & Alivisatos, A. P. Pyramidal and chiral groupings of gold nanocrystals assembled using DNA scaffolds. *J. Am. Chem. Soc.* **131,** 8455–8459 (2009).
12. Chen, W. *et al.* Nanoparticle superstructures made by polymerase chain reaction: collective interactions of nanoparticles and a new principle for chiral materials. *Nano Lett.* **9,** 2153–2159 (2009).

13. Sharma, J. *et al.* Control of self-assembly of DNA tubules through integration of gold nanoparticles. *Science* **323,** 112–116 (2009).
14. Chen, C.-L. & Rosi, N. L. Preparation of unique 1-D nanoparticle superstructures and tailoring their structural features. *J. Am. Chem. Soc.* **132,** 6902–6903 (2010).
15. Rothemund, P. W. K. Folding DNA to create nanoscale shapes and patterns. *Nature* **440,** 297–302 (2006).
16. Douglas, S. M. *et al.* Self-assembly of DNA into nanoscale three-dimensional shapes. *Nature* **459,** 414–418 (2009).
17. Fan, Z. & Govorov, A. O. Plasmonic circular dichroism of chiral metal nanoparticle assemblies. *Nano Lett.* **10,** 2580–2587 (2010).
18. Schaaff, T. G. & Whetten, R. L. Giant gold–glutathione cluster compounds: intense optical activity in metal-based transitions. *J. Phys. Chem. B* **104,** 2630–2641 (2000).
19. Shemer, G. *et al.* Chirality of silver nanoparticles synthesized on DNA. *J. Am. Chem. Soc.* **128,** 11006–11007 (2006).
20. George, J. & Thomas, K. G. Surface plasmon coupled circular dichroism of Au nanoparticles on peptide nanotubes. *J. Am. Chem. Soc.* **132,** 2502–2503 (2010).
21. Guerrero-Martínez, A. *et al.* Intense optical activity from three-dimensional chiral ordering of plasmonic nanoantennas. *Angew. Chem. Int. Edn Engl.* **50,** 5499–5503 (2011).
22. Guerrero-Martínez, A., Alonso-Gómez, J. L., Auguié, B., Cid, M. M. & Liz-Marzán, L. M. From individual to collective chirality in metal nanoparticles. *NanoToday* **6,** 381–400 (2011).
23. Berova, N., Nakanishi, K. & Woody, R. W. *Circular Dichroism: Principles and Applications* 2nd edn (Wiley-VCH, 2000).
24. Tørring, T., Voigt, N. V., Nangreave, J., Yan, H. & Gothelf, K. V. DNA origami: a quantum leap for self-assembly of complex structures. *Chem. Soc. Rev.* **40,** 5636–5646 (2011).
25. Fan, Z. & Govorov, A. O. Helical metal nanoparticle assemblies with defects: plasmonic chirality and circular dichroism. *J. Phys. Chem. C* **115,** 13254–13261 (2011).
26. Schreiber, R. *et al.* DNA origami-templated growth of arbitrarily shaped metal nanoparticles. *Small* **7,** 1795–1799 (2011).
27. Pilo-Pais, M., Goldberg, S., Samano, E., LaBean, T. H. & Finkelstein, G. Connecting the nanodots: programmable nanofabrication of fused metal shapes on DNA templates. *Nano Lett.* **11,** 3489–3492 (2011).
28. Halas, N. J., Lal, S., Chang, W.-S., Link, S. & Nordlander, P. Plasmons in strongly coupled metallic nanostructures. *Chem. Rev.* **111,** 3913–3961 (2011).
29. Urzhumov, Y. A. *et al.* Plasmonic nanoclusters: a path towards negative-index metafluids. *Opt. Express* **15,** 14129–14145 (2007).
30. Pendry, J. B. A chiral route to negative refraction. *Science* **306,** 1353–1355 (2004).

Supplementary Information is linked to the online version of the paper at www.nature.com/nature.

Acknowledgements We thank H. Dietz and G. Acuna for experimental advice and B. Yurke, E. Graugnard, J. O. Rädler and J. P. Kotthaus for discussions. We acknowledge J. Buchner and M. Rief for giving us access to their CD spectrometers, E. Herold for help with the CD measurements, and T. Martin and S. Kempter for assistance. We also thank D. M. Smith for carefully reading the manuscript. This work was funded by the Volkswagen Foundation, the DFG Cluster of Excellence NIM (Nanosystems Initiative Munich) and the NSF (USA).

Author Contributions A.K., R.S., A.H., F.C.S., A.O.G. and T.L. designed the research. A.K., R.S. and E.-M.R. designed the nanostructures and performed CD measurements. G.P. produced and purified gold samples. A.H. and T.L. investigated ORD effects. Z.F. and A.O.G. performed theoretical calculations. A.K., R.S. and A.O.G. prepared the figures and A.K., R.S., A.H., F.C.S., A.O.G. and T.L. wrote the manuscript.

Author Information Reprints and permissions information is available at www.nature.com/reprints. The authors declare no competing financial interests. Readers are welcome to comment on the online version of this article at www.nature.com/nature. Correspondence and requests for materials should be addressed to T.L. (tim.liedl@lmu.de).